A Pivot-Hinge-Style DNA Immobilization Method with Adaptable Surface Concentration Based on Oligodeoxynucleotide-Phosphorothioate Chemisorption on Gold Surfaces

Yoshinaga, Hisao
Department of Applied Chemistry, Faculty of Engineering, Kyushu University

Nakano, Koji
Department of Applied Chemistry, Faculty of Engineering, Kyushu University

Soh, Nobuaki
Department of Agriculture, Saga University

Ishimatsu, Ryoichi
Department of Applied Chemistry, Faculty of Engineering, Kyushu University

他

出版情報：Analytical Sciences. 28 (11), pp.1059-1064, 2012-11-10. 公益社団法人日本分析化学会
バージョン：

ANALYTICAL SCIENCES NOVEMBER 2012, VOL. 28

Original Papers

A Pivot-Hinge-Style DNA Immobilization Method with Adaptable Surface Concentration Based on Oligodeoxynucleotide-Phosphorothioate Chemisorption on Gold Surfaces

Hisao YOSHINAGA,* Koji NAKANO,*† Nobuaki SOH, Ryoichi ISHIMATSU,* and Toshihiko IMATO***

**Department of Applied Chemistry, Faculty of Engineering, Kyushu University, 744 Motooka, Nishi, Fukuoka 819-0395, Japan*
***Department of Agriculture, Saga University, 1 Honjo, Saga 840-8502, Japan*

The chemisorption of oligodeoxynucleotide phosphorothioate (s-oligo) is reported. A series of s-oligo DNAs was designed for use as capture probe DNA molecules. The s-oligo DNAs consist of the K-*ras* gene (5′-GGA GCT GGT GGC-3′) and a dodecamer deoxyriboadenosine, both of which lie on either side of an s-oligo DNA sequence. By primarily focusing on the capture probe DNA having five-successive s-oligo sequences, **e37**, the immobilization chemistry of **e37** was examined; atomic force microscopy achieved the direct visualization of individual molecules on Au(111) substrates, while a series of surface analyses, including IR, ellipsometry, and microgravimetry, showed that the s-oligo functional groups played a pivotal role in the surface-adlayer through the gold-thiol interaction. Interestingly, the amount of immobilization showed a definite relationship with the number of s-oligo linkages introduced, which should be important to regulate the concentration of the capture probe DNA molecules on the surface. Some preliminary studies using ferrocene-modified complementary sequences indicated that electrochemical labeling and readouts were possible.

(Received September 13, 2012; Accepted October 9, 2012; Published November 10, 2012)

Introduction

With remarkable richness, solid-phase nucleic acid hybridization has been of major importance in The Human Genome Project by yielding practical results.[1] They include monitoring gene expression, polymorphism analysis, clinical diagnosis, and also nucleic acid sequencing. These methods often use some sort of nucleic-acid probe immobilized on a solid-support or a transducer for the sake of hybridization.[2] Therefore, it has been acknowledged that one of the critical attributes for such kinds of analysis device to be workable lies in rational surface design, including immobilization chemistry. A number of methods have so far been developed to impart to the transducer surface a unique molecular recognition property of DNAs. They consist of broad-ranging surface treatments that can be placed in two groups; direct on-surface nucleic acid synthesis for the hybridization probe with a particular base sequence or after-the-synthesis immobilization.[3] In the case of any massively parallel analysis device, the former approach, *e.g*., high-density DNA arrays, is better suited, while the counterpart has been enjoying excellent flexibility, meeting with the needs of applications, such as DNA hybridization biosensors.[4-7]

Currently, the popular post-synthesis immobilization methods include: (1) biotinylated oligodeoxynucleotides (ODNs) captured by streptavidin-modified substrates,[8,9] (2) primary-amine-modified ODNs for reactions at carboxylate-modified substrates,[10-12] (3) alkanethiol-modified ODNs *via* chemisorption,[13-16] thioalkylation,[17,18] disulfide formation,[19,20] and (4) acrylamide-modified ODNs to form a thioether link.[21] These techniques are typically attained by chemical derivatization of the phosphate group at either the 5′- or 3′-terminus to form a covalent bond at the substrate surface. On the other hand, a couple of alternatives akin to the terminal modification methods have become realistic to impart to the ODNs some sort of chemical reactivity.[22] For example, various linkers are site-specifically attached to the nucleic-acid-framework, *e.g*., the C5 and C4 positions of the pyrimidines, the exocyclic amino groups and C8 positions of the purines, and the 2′-hydroxyl group of the carbohydrate residues.

On the other hand, the internucleotide phosphodiester linkage can be converted into the corresponding phosphorothioate function, *i.e*., s-oligo, in an automated DNA synthesis cycle.[23] Although this type of modification was originally developed for antisense oligonucleotide technologies,[24] we found that the particular derivative spontaneously forms self-assemblies on gold surfaces through chemisorption.[25] The technique represents DNA-backbone modification, and therefore allows us to arbitrarily assign the number as well as the location of the phosphorothioate function in the corresponding DNA sequence. If one treats only the interior phosphodiester links and the others are left untreated, the resulting surface-attached probe DNAs can offer a bimodal hybridization capability; the phosphorothioates functions play the pivotal role to attach the entire molecule to liberate the native chains for the specific molecular-recognition events. Hypothetically speaking, the native sequences may even act co-instantaneously, yet cooperatively, through rational molecular design, *e.g*., molecular beacon DNAs. This will bring some advantages over the

† To whom correspondence should be addressed.
E-mail: nakano@cstf.kyushu-u.ac.jp

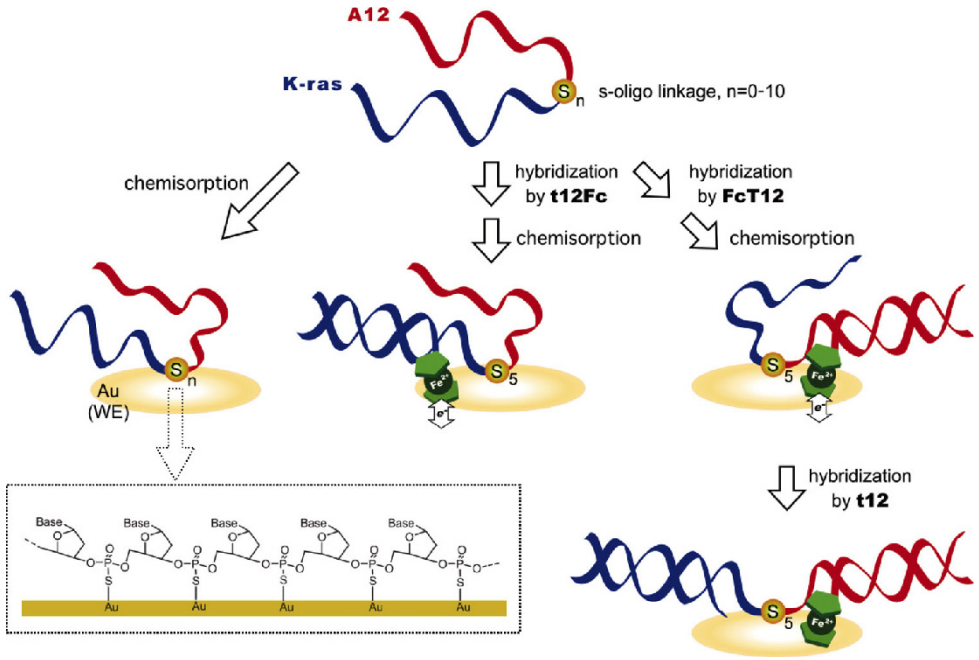

Fig. 1 Schematic illustration of the covalent attachment of the model capture probe DNA molecule, oligodeoxynucleotide phosphorothioate (s-oligo), or its corresponding half-hybridized species formed with a ferrocene-modified complementary DNA. In the box is shown the expected surface structure of the s-oligo surface-adlayer.

terminal modification methods.

In the present paper, the s-oligo-based immobilization chemistry was examined in detail (Fig. 1). We designed a model capture probe DNA that consists of the K-*ras* gene (codon 10 – 13, 5′-GGA GCT GGT GGC-3′) and a dodecamer deoxyriboadenosine, both of which were connected by a deoxythymidine-phosphorothioate chain. We initially focused on the pentamer phosphorothioate DNA probe, **e37**; various surface analytical methods including atomic force microscopy (AFM), IR spectroscopy, ellipsometry, and microgravimetric analysis using a quartz-crystal microbalance (QCM) characterized the **e37** molecular aggregates at the gold substrate surfaces. When we varied the s-oligo chain-length in the range from 0 (native) to 10, the surface concentration showed a marked dependence on the chain length. Therefore, the present immobilization was expected to be useful for regulated immobilization of the capture probe DNA molecules. Finally, some electrochemical-labeling applications for the **e37** probe DNA were examined. We selected two-kinds of half-hybridized species; one of the recognition sites is hybridized with the complementary sequence modified by ferrocene, while the counterpart is left unoccupied. We applied them for chemical modification of the gold electrode surfaces, and electrochemically characterized them. Some preliminary studies indicated that electrochemical labeling of the capture probe DNA molecules and readouts of the hybridization event were possible.

Experimental

Biogenic substances and chemical reagents

The DNA sequences were obtained from a custom synthesis by Sigma Genosys (Sapporo, Japan) and were used as received (Table 1). Synthesis of the ferrocene-modified dodecamer deoxyribothymine (**FcT12**) was made by the covalent coupling of *N*-(ferrocenecarbonyloxy)succinimide with the 5′-amino-modified deoxyribothymine dodecamer.[24,26] Similarly, the complementary sequence of K-*ras* was modified with ferrocene and was used as the model-target DNA (**t12Fc**). Each DNA sequence was dissolved in 50 mM phosphate buffer (pH 7) containing 100 mM NaCl to give a solution with a concentration of 100 μM (1 M = 1 mol dm^{-3}). For the electrochemical measurements, the capture probe DNA molecule, **e37**, was first hybridized with either **FcT12** or **t12Fc**. All chemical reagents were used as received.

Table 1 Base sequences for the deoxyoligonucleotide

Abbr.	Sequences (5′ to 3′)
e32	AAA AAA AAA AAA-$(TC)_2$-$(TC)_2$-GGA GCT GGT GGC
e33	AAA AAA AAA AAA-$(TC)_2$-Ts-$(TC)_2$-GGA GCT GGT GGC
e35	AAA AAA AAA AAA-$(TC)_2$-Ts_3-$(TC)_2$-GGA GCT GGT GGC
e37	AAA AAA AAA AAA-$(TC)_2$-Ts_5-$(TC)_2$-GGA GCT GGT GGC
e39	AAA AAA AAA AAA-$(TC)_2$-Ts_7-$(TC)_2$-GGA GCT GGT GGC
e42	AAA AAA AAA AAA-$(TC)_2$-Ts_{10}-$(TC)_2$-GGA GCT GGT GGC
FcT12	Fc-TTT TTT TTT TTT
t12Fc	GCC ACC AGC TCC-Fc

The s-notation denotes the phosphorothioester linkage. The covalently bound ferrocene function is abbreviated as Fc.

Characterization of DNA-adlayer

For IR measurements, polycrystalline Au films resistively deposited onto Tempax® glass substrates (Kinoene Kogaku, Japan; Au thickness, 2000 ± 200 Å) were used as the substrates. The substrate was chemically etched using a piranha solution (*caution! Piranha solution is a strong oxidizing agent and extreme care is necessary*) for pretreatment and then, the DNA solution (5 μM, 150 μL) was cast onto the chemically etched substrate. The substrate was stored in an airtight vessel to

prevent drying and left to the surface-adlayer development for 24 h at 5°C. FTIR-RAS (reflection absorption spectroscopy) was performed on a FTIR 620 V spectrometer (JASCO Co., Japan).[27] The thickness of the **e37** chemisorption layers was analyzed on an ellipsometer (Japan Laser Co., Japan) equipped with a He–Ne laser (5 mW, 632.8 nm) as a light source. The sample preparations were made by the same manner as IR. Microgravimetric analysis was performed using a QCA917 or a 934 sensing system (Seiko Instruments Inc., Japan). Commercially available gold QCM-chips (QA-A9M-AU) were used for measurements. For AFM, evaporated gold films with a (111) texture were used as the substrate (Agilent Technologies, Inc., CA). AFM imaging was performed using a JSPM-4210 scanning probe microscope (JEOL, Tokyo, Japan). The instrument was operated in the non-contact mode imaging with frequency-modulation detection. A version of the public domain image analysis software NIH Image, Image SxM processed the topographic images of the sample surface. Silicon cantilevers (k = 14.0 N/m, f_0 = 315 kHz, r = 10 nm) purchased from MikroMasch (Tallinn, Estonia) were used throughout the study.[28]

Electrochemical measurements

Gold disk electrodes (BAS Co., Japan. ϕ1.6 mm) were polished with alumina slurries of successively finer grades (Buehler Co.) and were cleaned by ultrasonication in deionized water. The surface modification was made with the half hybridized species of **e37** (**e37/FcT12** or **e37/t12Fc**) using the same procedure described above. The DNA-modified electrode was gently rinsed with 1 M $NaClO_4$ repeatedly and subsequently rinsed with deionized water. An ALS 750D electrochemical analyzer (BAS Co., Japan) was used for cyclic voltammetric measurements in combination with a single-compartment electrochemical cell; a platinum wire was employed as the auxiliary electrode and the electrode potential was measured with reference to a Ag/AgCl (3 M NaCl) electrode. The gold QCM-chip mounted into a solution cell served as the working electrode in the case of the QCM-coupled hybridization measurements. All measurements were made at ambient temperature, typically 22 – 25°C.

Results and Discussion

*AFM imaging of **e37** molecular aggregates and surface topological characterization*

Various methods of surface analysis have been used to characterize the self-assemblies of terminally-thiolated capture probe DNA molecules formed at the gold substrate surface. They include IR spectroscopy,[26] x-ray photoelectron spectroscopy,[15] surface plasmon resonance,[16] and microgravimetry analysis.[8,9] AFM imaging has also been used to address the height of the self-assemblies primarily based on the scratch-and-height determination technique.[29,30] These types of experiments have been used to detect DNA hybridization by comparing various surface parameters, *e.g.*, smoothness,[31] height,[32,33] and density.[34] We have also reported single-molecule imaging of a molecular-beacon DNA self-assembly to achieve target DNA detection through visualizaton.[28,35] Among them, by varying the concentration of the s-oligo DNA solution used for self-assembly, we obtained a series of AFM images that showed a definite relationship between the specific surface roughness and the s-oligo DNA concentration. The AFM-based strategy characterized the **e37** molecular aggregates as summarized below.

The high-resolution AFM imaging produced unambiguous images for the Au(111) substrates whose surfaces were modified

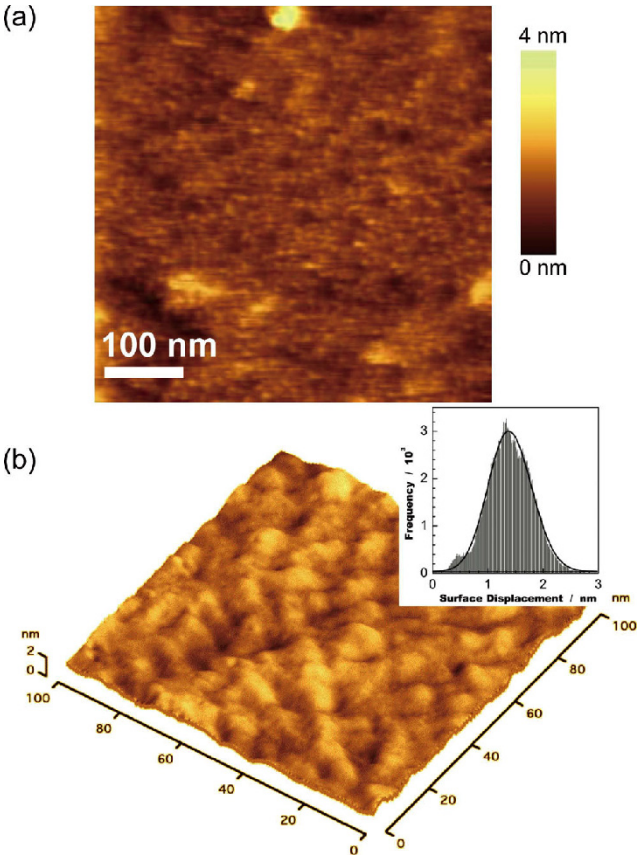

Fig. 2 Representative topographical image of Au(111) substrates treated by **e37** at 500 × 500 nm resolution (a) and a high-resolution image with 3D-expression (b). The inset shows a histogram for the surface roughness data, showing the result of non-linear curve fitting (solid line).

by **e37** (Fig. 2); physical matter is finely distributed almost completely over the substrate surface. The surface adsorbates are commonly found as curled or tangled rope-like entities with specific lengths of *ca.* 30 – 40 nm. We can estimate a specific length of 27 nm for a 37-mer DNA in its ladder conformer. AFM images of the untreated bare Au substrate surfaces displayed atomically flat (111) grains with pronounced step edges. In addition, as AFM images typically consist of a set of pixels into which specific height data are encoded, this particular feature afforded us a detailed roughness analysis for the particular surface structure. The result of a simple histogram analysis is also shown in Fig. 2. The histogram plots show that a frequency distribution fundamentally traces a specific curve typical of a normal distribution. Based on a nonlinear curve fitting of the plots, assuming either a single Gaussian function peak or an asymmetrical peak, it was determined that the height of the surface object as a representative value of the surface displacement was 1.4 nm. Based on a Corey–Pauling–Koltun (CPK) model constructed for **e37**, it was estimated that the representative axial section length of the single-stranded DNA in the stepladder conformation was 1.2 nm. Both data agreed fairly well with each other. Based on these results, we concluded that each rope-like entity observed in Fig. 2 represents a single **e37** DNA strand.

*Characterization of **e37** adlayer by FTIR-RAS*

FTIR-RAS measurements on the Au substrates containing **e37**

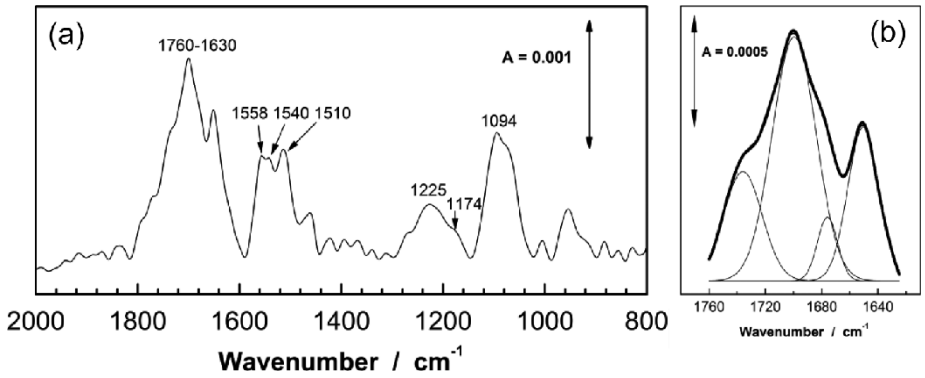

Fig. 3 FTIR reflection-absorption spectrum of a Au substrate treated by **e37** (a). In (b), the results for the quantitative curve-fitting analysis for the –C=O region are shown (thin lines), while their sum total (thick line) reproduces the original data well.

molecular aggregates confirmed that the surface phases formed reflected the intended adsorbates. Figure 3 shows a representative FTIR-RAS spectrum for an **e37**-treated gold substrate. By reference to the structural features of nucleic acids, two peaks at 1225 and 1174 cm^{-1} were assigned as anti-symmetric and symmetric P–O stretches of the phosphate group, respectively. The peak at around 1094 cm^{-1} was identified as the deoxyribose C–O–C stretch of the backbone. A broad band consisting of components at 1558, 1540, and 1510 cm^{-1} was assigned as the absorption of the purine skeleton. Last, the intense peaks between 1760 – 1630 cm^{-1} were ascribed as C=O stretches. An *ab initio* calculation for the nucleobases on Gaussian 03 code using the HF/STO-3G basis set showed that the specific strength of the C=O bond takes the order of guanine > thymine with two-kinds of C=O groups > cytosine. Now, a theoretical waveform analysis has shown that this particular absorption band could be further deconvoluted to give four-distinct absorptions, which we assigned to be 1736 cm^{-1} for the C=O function in guanine, 1700 and 1676 cm^{-1} for thymine, 1651 cm^{-1} for cytosine, respectively. The waveform analysis also reported normalized intensities for guanine, thymine and cytosine of 20, 58, and 22%, respectively. The specific intensity ratio of 1:3:1 reproduced the nucleobase-content of **e37**: namely, seven-fold dG, eleven-fold dT, and six-fold dC, respectively.

Determination of film thickness by ellipsometry

Ellipsometry measurements have analyzed the thickness of the **e37** adlayers. We followed the conventional procedure by adopting an air–organic film–substrate three-layer model and assumed a uniform film thickness with a refractive index of 1.45.[15] Using an iterative procedure (least-square minimization), unknown optical constants and/or thickness parameters were varied to determine the parameter set that best matched the experimental data. We collected them at 22 randomly chosen zones, which varied over the range from 0.7 to 2.4 nm. Statistical analysis determined the film thickness to be 1.6 ± 0.33 nm, which was slightly larger than that determined by the AFM examinations (1.4 nm). The flexible **e37** chains in the single-stranded state tend to pile up upon each other when they adopt a horizontally aligned structure at the surface. This may add some excess for the film thickness data.

Characterization by microgravimetric analysis using QCM

For various types of terminally thiolated DNAs, microgravimetric analysis using a QCM has been effective when characterizing their immobilization chemistry as well as hybridization capability with their target DNA. We applied the procedure to the s-oligo immobilization method for determining the amount of adsorption. Interestingly, by changing the number of the s-oligo linkage and comparing the amount of adsorption, we found a definite relationship between them.

Upon **e37** chemisorption, we observed specific resonant frequency decreases, which are equivalent to 14 ± 5.2 pmol cm^{-2} ($n = 10$) of the surface concentration when Sauerbrey's equation is adopted. The particular data seems to be considerably larger than that which is expected from the cross-section of **e37** in the linear (32 nm^2) or circularly curved conformation (58 nm^2) whose reciprocal is equivalent to the theoretical data. Similarly, the CPK model showed five successive nucleotides with a footprint of 4.2 nm^2, which leads to a theoretical surface concentration of 39 pmol cm^{-2}. These simple estimations suggest that the s-oligo chemisorption occurs primarily only at the phosphorothioate sequences. Currently, terminally-thiolated single-stranded DNA probes have been acknowledged to attain values of typically a few tens of picomoles per unit area DNA up to one-hundred picomoles per unit area DNA attached to the Au substrate surface. Therefore, it can be concluded from the present backbone modification method that the particular adsorbates possess an adequate affinity for chemisorption, which compares well with the mainstream approaches.

We next examined the effect of the number of gold-sulfur interactions upon the surface concentration by varying the number of phosphorothioate functional groups (Fig. 4). Interestingly, the capture probe DNA molecules could be adsorbed on the Au substrate, albeit in a rather small, but distinct quantity, irrespective of the s-oligo sequence (**e32**) used. As previously reported by Letsinger's group,[36] Whitman's group,[37] and Georgiadis's group,[38] some sort of single-stranded DNA probes are chemisorbed by the specific interaction of the nucleobase, especially adenine, with the underlying Au substrate. The adenine-Au affinity reaction is considered to be one of the causes of the **e32** adsorption. The adsorption of the capture probe DNA molecules was subsequently enhanced to a considerable extent by the phosphorothioate modification, even though only single dTs were involved (**e33**). Then, the amount of immobilization monotonically increased with increasing number of s-oligo functional groups; the stability of the s-oligo surface adsorbates could be enhanced through multiple Au-thiol bonding interactions with the Au substrate.

Beyond the heptamer conversion, however, the amount of immobilization drastically decreased by less than one half of the

maximum value (**e42**). This may be explained by the steric hindrance of the anchoring sequence; in the tetrahedral arrangement of the phosphorothioate-bridge, every thiolate group by necessity, takes the face-to-face arrangement with the underlying Au atoms, and this unfavorable strain could cause instable adsorption. Regarding the surface state of the capture probe DNA molecules, efficient binding with the target DNA occurs when the DNA probes are vertically immobilized with sufficient clearance. Previously, Opdahl and coworkers reported a density-controlled grafting method of single-stranded DNA probes; by introducing anchoring sequences of adenine nucleotides with different lengths, they prepared the DNA-attached Au substrates with varied surface concentrations ranging from 2×10^{13} to 3.5×10^{13} DNA-strands per unit area.[39] The present s-oligo immobilization method will also realize the opportunities of covalent-attachment with a controlled surface-concentration of capture probe DNA molecules.

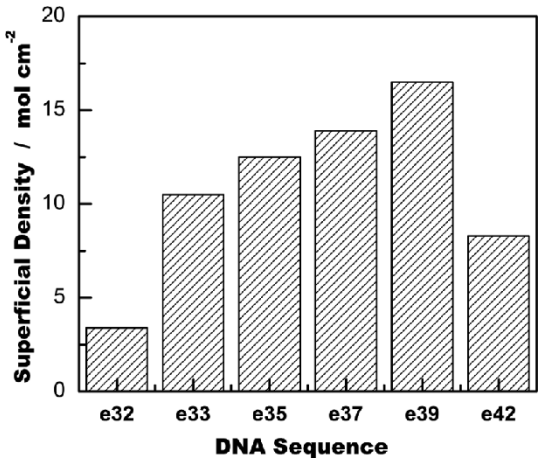

Fig. 4 Dependence of the amount of adsorption of the capture probe DNA molecules upon the number of phosphorothioate functional groups in the corresponding nucleobase sequences. The results obtained for three different sample preparations were averaged and plotted for each capture probe DNA molecule.

Electrochemical-labeling applications

Finally, we examined some electrochemical labeling/readout applications using the **e37**-modified Au electrodes as an example. First, **e37** was hybridized with **t12Fc**, which represents one of the complementary sequences, and the resulting half-hybridized species, **e37/t12Fc**, was attached onto the Au electrode. The cyclic voltammogram (CV) for the **e37/t12Fc**-modified Au electrode obtained in an electrolytic solution is shown in Fig. 5(a). Although the corresponding CV suffers from intense background current, the oxidative wave was identified at +0.3 V, which was reasonably explained by the oxido-reduction of ferrocene. On the other hand, the enormously large background current made the reduction current indiscernible. The magnitude of the oxidative current increased linearly as the scan-rate increased, indicating the surface process. By integrating the current under the oxidation peak, we obtained the amount of **e37/t12Fc** at the electrode surface to be 22 pmol cm^{-2}; the calculated amount from the electrochemical measurements was slightly higher than expected, but agreed fairly well with that from the QCM measurements. As expected, the bare Au electrodes only gave capacitive currents in the potential range used in the present study.

For comparison, **e37** was hybridized with **FcT12**, which is another complementary sequence, and the resulting **e37/FcT12** was used in the same manner as **e37/t12Fc**. Here, we used the Au-QCM substrate as the working electrode, and the

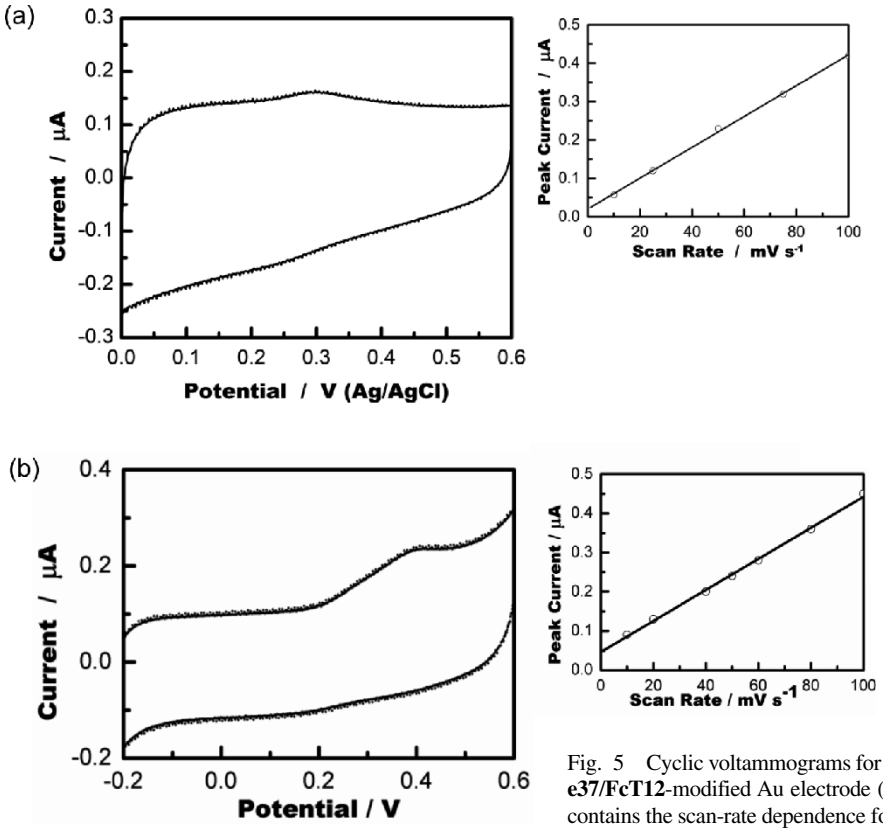

Fig. 5 Cyclic voltammograms for the **e37/t12Fc**-modified Au electrode (a) and the **e37/FcT12**-modified Au electrode (b) in 0.1 M KCl at 50 mV s^{-1}. Each panel also contains the scan-rate dependence for the magnitude of the oxidation peak current.

electrochemical measurements were combined with the microgravimetric measurements. Again, we obtained CVs having delicate current features at around +0.35 – 0.4 V, which enhanced linearly as the scan-rate increased (Fig. 5(b)). The surface concentration of **e37/FcT12** calculated by the quantity of electric charge was 8.3 pmol cm^{-2}. Although **e37/FcT12** showed rather weak chemisorption compared with **e37/t12Fc**, it fell within the margin of error obtained for **e37** chemisorption. Therefore, the s-oligo immobilization method will provide opportunities of an interconvertible-style electrochemical labeling at either of the recognition sequences.

In-situ QCM analysis determined that the mass increase for **e37/FcT12** chemisorption was equivalent to 8.1 pmol cm^{-2}, which agreed well with the electrochemical data. When the **e37/FcT12**-modified QCM chip was treated with **t12** for hybridization, the specific mass increase was determined to be 3.2 pmol cm^{-2}. The probe/target binding attained a hybridization efficiency of 40%, which is in general agreement with that of previously reported results.[16] Interestingly, the oxidative wave of **e37/FcT12** was considerably reduced upon **t12** hybridization. The electrochemically-inactive target DNA may cause the electrode reaction of the label DNA to be sluggish (data not shown). We are currently investigating this phenomenon to gain a deeper understanding, since the benefits of this technology would be useful for applications of a non-label hybridization biosensor.

Acknowledgements

We thank Prof. A. Takahara and Dr. M. Kobayashi of Kyushu University for access to the ellipsometer and their technical assistance. K. N. acknowledges financial support from a Grant-in-Aid for Scientific Research from the Ministry of Education, Culture, Sports, Science and Technology (MEXT), Japan. This work was also supported by the Kyushu University Global COE Program—Science for Future Molecular Systems (H. Y.), and the Nanotechnology-Support Network Program in Kyushu Area (K. N.).

Supporting Information

Synthetic procedures and analytical data. This material is available free of charge on the Web at http://www.jsac.or.jp/analsci/.

References

1. T. A. Brown, "*Genomes 3*", **2006**, Garland Science, UK.
2. G. Hardiman, "*Microarray Innovations: Technology and Experimentation*", **2009**, CRC Press, Boca Raton.
3. W. Christine, "*Topics in Current Chemistry 261: Immobilisation of DNA on Chips II*", **2005**, Springer, Berlin.
4. T. G. Drummond, M. G. Hill, and J. K. Barton, *Nat. Biotechnol*., **2003**, *21*, 1192.
5. I. Willner and M. Zayats, *Angew. Chem., Int. Ed*., **2007**, *46*, 6408.
6. A. Sassolas, B. D. Leca-Bouvier, and L. J. Blum, *Chem. Rev*., **2008**, *108*, 109.
7. F. R. R. Teles and L. P. Fonseca, *Talanta*, **2008**, *77*, 606.
8. R. C. Ebersole, J. A. Miller, J. R. Moran, and M. D. Ward, *J. Am. Chem. Soc*., **1990**, *112*, 3239.
9. F. Caruso, E. Rodda, D. N. Furlong, K. Niikura, and Y. Okahata, *Anal. Chem*., **1997**, *69*, 2043.
10. S. R. Rasmussen, M. R. Larsen, and S. E. Rasmussen, *Anal. Biochem*., **1991**, *198*, 138.
11. K. Lindroos, U. Liljedahl, M. Raitio, and A.-C. Syvänen, *Nucleic Acids Res*., **2001**, *29*, e69.
12. S. J. Oh, S. J. Cho, C. O. Kim, and J. W. Park, *Langmuir*, **2002**, *18*, 1764.
13. M. Maeda, Y. Mitsuhashi, K. Nakano, and M. Takagi, *Anal. Sci*., **1992**, *8*, 83.
14. Y. Okahata, M. Matsunobu, K. Ijiro, M. Mukae, A. Murakami, and K. Makino, *J. Am. Chem. Soc*., **1992**, *114*, 8299.
15. T. M. Herne and M. J. Tarlov, *J. Am. Chem. Soc*., **1997**, *119*, 8916.
16. A. W. Peterson, R. J. Heaton, and R. M. Georigiadis, *Nucleic Acids Res*., **2001**, *29*, 5163.
17. L. A. Chrisey, G. U. Lee, and C. E. O'Ferrall, *Nucleic Acids Res*., **1996**, *24*, 3031.
18. J. M. Brockman, A. G. Frutos, and R. M. Corn, *J. Am. Chem. Soc*., **1999**, *121*, 8044.
19. Y.-H. Rogers, P. Jiang-Baucom, Z.-J. Huang, V. Bogdanov, S. Anderson, and M. T. Boyce-Jacino, *Anal. Biochem*., **1999**, *266*, 23.
20. R. Lenigk, M. Carles, N. Y. Ip, and N. J. Sucher, *Langmuir*, **2001**, *17*, 2497.
21. L. M. Demers, D. S. Ginger, S.-J. Park, Z. Li, S.-W. Chung, and C. A. Mirkin, *Science*, **2002**, *296*, 1836.
22. S. M. Hecht, "*Bioorganic Chemistry: Nucleic Acids*", **1996**, Oxford University Press, New York.
23. R. P. Iyer, W. Egan, J. B. Regan, and S. L. Beaucage, *J. Am. Chem. Soc*., **1990**, *112*, 1253.
24. T. Ihara, M. Nakayama, M. Murata, K. Nakano, and M. Maeda, *Chem. Commun*., **1997**, 1609.
25. A. Bardea, F. Patolsky, A. Dagan, and I. Willner, *Chem. Commun*., **1999**, 21.
26. M. Nakayama, T. Ihara, K. Nakano, and M. Maeda, *Talanta*, **2002**, *56*, 857.
27. K. Nakano, T. Yoshitake, Y. Yamashita, and E. F. Bowden, *Langmuir*, **2007**, *23*, 6270.
28. K. Nakano, H. Yamanouchi, H. Yoshinaga, N. Soh, and T. Imato, *Chem. Commun*., **2010**, *46*, 5683.
29. S. O. Kelly, J. K. Barton, N. M. Jackson, L. D. McPherson, A. B. Potter, E. M. Spain, M. J. Allen, and M. G. Hill, *Langmuir*, **1998**, *14*, 6781.
30. D. Zhou, K. Sinniah, C. Abell, and T. Rayment, *Langmuir*, **2002**, *18*, 8278.
31. M. Holmberg, A. Kühle, J. Garnæs, and A. Boisen, *Ultramicroscopy*, **2003**, *97*, 257.
32. D. Zhou, K. Sinniah, C. Abell, and T. Rayment, *Angew. Chem., Int. Ed*., **2003**, *42*, 4934.
33. C. E. Immoos, S. J. Lee, and M. W. Grinstaff, *ChemBioChem*., **2004**, *5*, 1100.
34. M. Liu and G.-Y. Liu, *Langmuir*, **2005**, *21*, 1972.
35. H. Yoshinaga, K. Nakano, N. Soh, and T. Imato, *Anal. Sci*., **2012**, *28*, 939.
36. J. J. Storhoff, R. Elghanian, C. A. Mirkin, and R. L. Letsinger, *Langmuir*, **2002**, *18*, 6666.
37. H. Kimura-Suda, D. Y. Petrovykh, M. J. Tarlov, and L. J. Whitman, *J. Am. Chem. Soc*., **2003**, *125*, 9014.
38. L. K. Wolf, Y, Gao, and R. M. Georgiadis, *Langmuir*, **2004**, *20*, 3357.
39. A. Opdahl, D. Y. Petrovykh, H. Kimura-Suda, M. J. Tarlov, and L. J. Whitman, *Proc. Natl. Acad. Sci., U. S. A*., **2007**, *104*, 9.